Physically Cross-Linked Alkylacrylamide Hydrogels: Phase Behavior and Microstructure

Jun Tian,[†,‡] Thomas A. P. Seery,[‡,§] and R. A. Weiss*[,†,‡]

Chemical Engineering Department, University of Connecticut, Storrs, Connecticut 06269; Polymer Program, Institute of Materials Science, University of Connecticut, Storrs, Connecticut 06269; and Chemistry Department, University of Connecticut, Storrs, Connecticut 06269

Received March 17, 2004; Revised Manuscript Received October 16, 2004

ABSTRACT: The volume phase transition and the microstructure of physically cross-linked hydrogels composed of either *N*,*N*-dimethylacrylamide (DMA) or *N*-isopropylacrylamide (NIPA) and 2-(*N*-ethylfluorooctanesulfonamido)ethyl acrylate, FOSA, were studied using differential scanning calorimetry (DSC), water swelling measurements (WS), and small-angle X-ray scattering (SAXS). DSC and WS measurements showed that FOSA/NIPA gels exhibited a volume phase transition (VPT) but that the FOSA/DMA gels did not. The temperature of the VPT (T_{VPT}) for the FOSA/NIPA gels was lower than that for the covalent NIPA gel, and T_{VPT} decreased and the transition broadened with increasing FOSA concentration. A peak in the SAXS structure factor indicated that the hydrophobic interactions promoted nanophase separation in both gels—in the dry and hydrated states.

Introduction

Hydrophobically modified water-soluble acrylamide polymers have a variety of applications, including viscosity thickeners,[1−4] microencapsulation,[5−8] biosensors[9,10] and controlled drug delivery.[11−18] The hydrophobic modification may involve copolymerization of an acrylate with an acrylamide or alkylacrylamide[5,13−15,17−24] or incorporation of a second alkylacrylamide containing a longer alkyl chain.[1,2,6,16,25,26]

The hydrophobic modification can significantly perturb the rheological properties and phase behavior of aqueous solutions. For example, aqueous solutions of copolymers of *N*-isopropylacrylamide (NIPA) with longer chain *N*-alkylacrylamides (NAA) exhibit lower critical solution temperature (LCST) behavior.[26,27] In general, the LCST decreases as the alkyl chain length becomes longer, i.e., as the hydrophobic nature of the polymer increases.[28] However, Ringsdorf et al.[26] reported that the LCST for aqueous solutions of NIPA−NAA copolymers with C_{18} alkyl groups was higher than for similar polymers with C_{14} alkyl chains, which they attributed to the formation of hydrophobic microdomains in the C_{18}-containing copolymers.

Hogen-Esch and co-workers[19,20,29] compared the solution properties of acrylamide (AM) copolymers modified by the incorporation of 2-(*N*-ethylperfluorooctane sulfonamido)ethyl acrylate, FOSA, with *n*-lauryl acrylate (LA)-modified AM. Although the concentrations of the fluorinated species in the fluorocarbon-modified AM copolymers were 1−2 orders of magnitude lower than that in the hydrocarbon analogues, the viscosities of aqueous solutions of the fluorine-containing polymers were 1−2 orders of magnitude higher than that for the hydrocarbon-containing AMs. They concluded that fluorocarbon hydrophobes were much more effective than hydrocarbon hydrophobes at promoting inter- or intramolecular associations.

Bae et al.[30] prepared hydrogels from copolymers of FOSA and NIPA or DMA using FOSA concentrations as high as 20 mol %. FOSA/AM and FOSA/DMA copolymers were previously synthesized by Hogen-Esch and co-workers,[19,23] and FOSA/NIPA copolymer were prepared by Li et al.,[31] but the FOSA concentration in those materials was restricted to below 1 or 2 mol % in order to maintain water solubility. Above a FOSA concentration of 5 mol % for FOSA/DMA or 2 mol % for FOSA/NIPA, the copolymers were insoluble in water because of the physical cross-links that arise from intermolecular associations of the hydrophobic species. The alkylacrylamide portion of the copolymer is still hydrophilic, and as a result, these copolymers form highly swollen hydrogels when immersed in water.

Chemically cross-linked polymer gels exhibit a reversible transition between a swollen and collapsed polymer phase, which is called a volume phase transition (VPT).[32,33] The VPT may be induced by environmental stimuli, such as changes in temperature,[34−36] pH,[8,37,38] solvent composition,[34,39−42] or exposure to light.[43,44] For example, polyNIPA gels in water undergo a VPT at 33.2 °C,[34] which is close to the LCST or θ-temperature of polyNIPA aqueous solutions (∼31 °C).[45,46] At the VPT, gel properties such as heat capacity and volume undergo transitions. Although the VPT is a first-order thermodynamic transition, experimentally it often is observed as a continuous transition because of the kinetics of solvent diffusion out of the gel.[47,48] Thermal property changes such as heat capacity may be measured by calorimetry,[49,50] and the volume change can be studied by swelling measurements.[33,51]

The hydrophobic modification generally reduces the VPT of hydrogels, e.g., copolymer gels of NIPA with hydroxyethyl methacrylate,[52] and increasing the gel hydrophilicity increases the VPT, e.g., NIPA−DMA copolymer gels.[53] The addition of an ionic species into an otherwise neutral gel also increases the VPT;[35,54−56] e.g., the copolymerization of 4.6 mol % acrylic acid with NIPA increased the VPT to 50.8 °C.[56]

Although much is known of the structure and properties of ionic and neutral covalent-cross-linked gels,

† Chemical Engineering Department.
‡ Institute of Materials Science.
§ Chemistry Department.
* Corresponding author: e-mail rweiss@mail.ims.uconn.edu.

10.1021/ma049475r CCC: $27.50
Published on Web 12/03/2004

Scheme 1. Structure of the Monomers Used

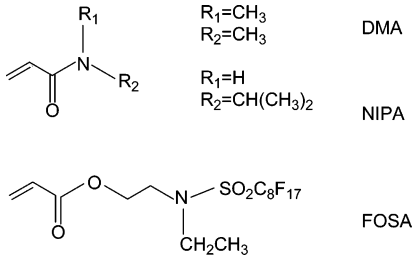

Table 1. Characterization Results of Polymers

polymer ID	FOSA[a] mol %	FOSA[a] wt %	DMA or NIPA (mol %)	T_g (°C)	M_w (10^4 Da)	M_n (10^4 Da)
polyFOSA			0	44.5		
polyDMA			100	124.0	8.6	3.8
DF5	4.9	25	95.1	110.7	7.3	3.8
DF9	9.0	38	91.0	99.6	5.6	2.9
DF17	16.5	56	83.5	94.8	7.7	3.4
DF22	21.5	63	78.5	88.8	7.6	5.1
polyNIPA			100	145.1	7.2	4.8
NF2	2.0	10	98	138.4	5.6	3.4
NF5	5.4	24	94.5	130.6	6.4	3.4
NF8	7.7	32	92.3	128.2	7.2	4.2
NF10	10.2	39	89.8	126.0	7.1	4.3

[a] The added FOSA content was in agreement with observed.[30]

relatively little is known about physical gels. For FOSA-modified NIPA or DMA gels, one might expect that at sufficiently high FOSA concentrations the hydrophobic interactions may also promote nanophase separation of the FOSA-rich domains. Therefore, the microstructure of these hydrogels may be more complicated than the analogous covalently cross-linked alkylacrylamides. This paper describes the effect of copolymerization of FOSA with DMA and NIPA on the phase behavior and microstructure of the resulting physically cross-linked hydrogels. A small-angle neutron scattering study is discussed in a second paper,[57] in which a model for the microstructure of these hydrogels is described.

Experimental Section

Materials. *N*,*N*-Dimethylacrylamide (DMA, 99%), *N*-isopropylacrylamide (NIPA, 99%), and 2-(*N*-ethylperfluorooctanesulfonamido)ethyl acrylate (FOSA) were obtained from Aldrich Chemical Co., Acros Chemical Co., and 3M Co., respectively. The structures of these monomers are shown in Scheme 1. Acetone (99.5%), tetrahydrofuran, THF (HPLC grade), and deuterium oxide, D_2O (99.8% d), were obtained from Fisher Scientific Co.

The synthesis of the FOSA/DMA and FOSA/NIPA copolymers was described elsewhere.[23,30,31] DMA was vacuum-distilled over calcium hydride (Acros, 93%) to remove the inhibitor, NIPA was recrystallized twice from a mixture of hexane (Fisher, CAS grade) and benzene (Fisher, 99%) (65/35 v/v), and FOSA was recrystallized three times from methanol (Fisher, 99.8%) before use. The initiator, 1,1′-azobis(isobutyronitrile), AIBN (Aldrich, 99%), was purified by recrystallization twice from methanol. The monomers and initiator were codissolved in 1,4-dioxane (Fisher, 99%), and the solution was degassed by purging with nitrogen for 30 min. The polymerization was run for 24 h at 60 °C, and then the solution was cooled to room temperature. The polymer was precipitated in excess diethyl ether (Fisher, 99%) or hexane and then dried, first at 60 °C for 24 h and then under vacuum at 100 °C overnight.

The copolymers that were synthesized and used in this study are summarized in Table 1. The composition of the copolymers was determined by ^{1}H NMR using d-chloroform as solvent (Fisher, 99.8% d), the glass transition was determined by differential scanning calorimetry, and the molecular weight averages were measured by gel permeation chromatography. The nomenclature used in this paper for the DMA/FOSA and NIPA/FOSA copolymers is DF*xx* and NF*xx*, respectively, where *xx* represents the mol % FOSA.

Table 2. Gel Characteristics

gel ID	monomer concn (mM)	cross-linker concn (mM)	vol fraction of network ϕ
DMA	503.1	22.3	0.068
NIPA	689.2	23.7	0.065

Chemical cross-linked NIPA and DMA gels were also prepared by redox polymerization for comparison with the NF and DF gels. *N*,*N*′-Methylene bis(acrylamide), BIS (Aldrich, 98%), was used as the cross-linker, *N*,*N*,*N*′,*N*′-tetramethylethylenediamine, TEMED (Aldrich, 99%), was used as the initiator, ammonium persulfate (Acros, CAS grade) was used as the accelerator, and deuterium oxide, D_2O (Fisher, 99.8% atom d), was used as the solvent. DMA (or NIPA), BIS, and ammonium persufate were codissolved in D_2O, degassed, and then kept in the refrigerator for ~30 min. TEMED was added to the solution to initiate the polymerization. The solution was then transferred to a reaction vessel, and the temperature was held at 20 °C using a Julabo F25 circulator. The polymerization was run for 24 h. Then the gel was washed with excess D_2O. The DMA and NIPA gel characteristics are listed in Table 2. Copolymer films, 0.5 mm thick, for the swelling and small-angle X-ray scattering measurements were prepared by compression-molding between 150 and 180 °C.

Gel Characterization. Equilibrium swelling measurements were made using compression-molded films that were dried and annealed at 150 °C under vacuum for 2 h before use. A preweighed specimen was immersed into deionized water that was controlled to within ±0.01 °C using a Julabo F25 temperature-controlled circulator. The gel was allowed to equilibrate at the test temperature, was patted dry with a tissue to remove surface water, and was then weighed to within ±1 mg to determine the equilibrium water concentration, which is given in this paper as the weight percent water sorption per dry polymer. The volume phase transition temperature (T_{VPT}) was calculated by fitting a standard sigmoidal four-parameter logistic equation

$$f(x) = \frac{d}{1 + \left(\frac{x}{b}\right)^a} + c \qquad (1)$$

and defining T_{VPT} as the inflection in the equilibrium water concentration at the transition of the gel from highly swollen to a collapsed state.

Thermal analysis of the volume phase transition was carried out with a TA Instruments, model Q100, differential scanning calorimeter (DSC). Gel samples were hermetically sealed in aluminum pans (KEmtec Lab Devices), and the samples were weighed before and after the DSC runs to confirm that no water was lost during the measurement. Since a slow heating rate, ~1 °C/min, was used to minimize the effect of transition kinetics,[58] the modulated-temperature DSC (MTDSC) mode was used to optimize the signal-to-noise ratio.

Small-angle X-ray scattering (SAXS) measurements were performed using a Rigaku rotating anode X-ray generator operating at 4 kW with Cu Kα radiation ($\lambda = 0.154$ nm) and a Ni filter. This was interfaced with a Bruker AXS SAXS system, including a Hi-Star area detector. The sample geometry used allowed for data collection over a range of scattering vector, q ($q = 4\pi \sin\theta/\lambda$, where λ = wavelength and θ = one-half the scattering angle), from 0.28 to 3.3 nm^{-1}. That q range corresponded to sizes in real space, d (where $d = 2\pi/q$), of 1.9−22 nm. Measurements were made on dry and water-swollen films. The hydrated samples were sandwiched between Kapton (DuPont) films to prevent the sample from dehydrating during the experiment. SAXS from DF gels was measured at ambient temperature, while SAXS from NF gels was obtained at

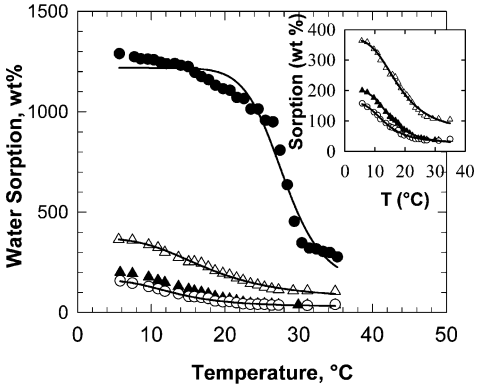

Figure 1. Equilibrium water sorption as a function of temperature for NF*xx* films: *xx* = 2 (●), 5 (△), 8 (▲), and 10 (○). The solid curve is the fit of eq 1.

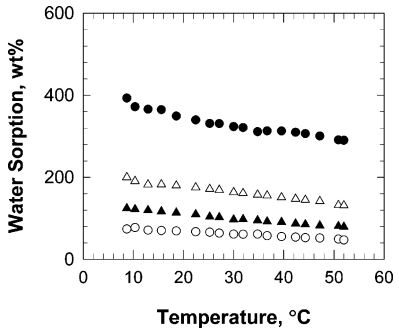

Figure 2. Equilibrium water sorption as a function of temperature for DF*xx* films: *xx* = 5 (●), 9 (△), 17 (▲), and 22 (○).

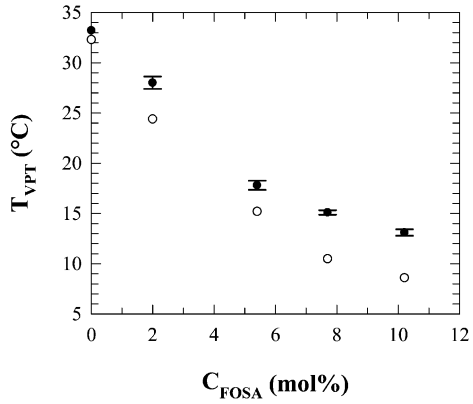

Figure 3. Volume phase transition as a function of FOSA concentration for NF gels: (●) equilibrium swelling experiments; (○) DSC experiments. The swelling value for the T_{VPT} for polyNIPA is from Hirokawa and Tanaka.[34]

10 °C, which was below the VPT temperature of all the samples. An ISTEC, model HCS410, hot stage with an INSTEC LN2 temperature controller was used to control the sample temperature. A background correction was made by subtracting the scattering from an empty cell, and the 2-dimensional data were circularly averaged to calculate $I(q)$.

Results and Discussion

Volume Phase Transition (VPT). The equilibrium water sorption as a function of FOSA concentration is shown in Figures 1 and 2 for the NF and DF hydrogels, respectively. Figure 1 shows that the NF gels exhibited a VPT. T_{VPT} is plotted against the FOSA concentration in the NF copolymer in Figure 3. T_{VPT} decreased, and the transition broadened with increasing FOSA concentration. In contrast to the NF gels, the water sorption

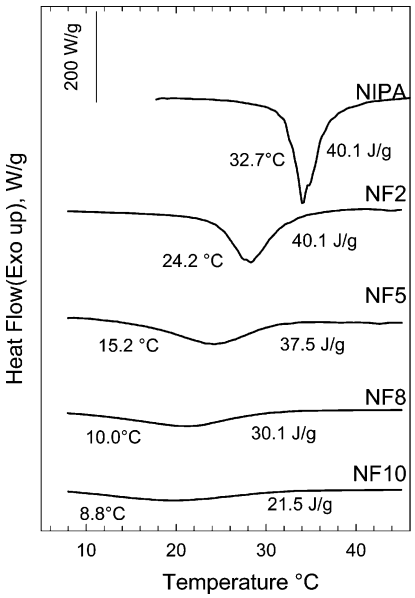

Figure 4. DSC heating thermograms for NIPA and NF gels. T_{VPT} was defined as the onset of the endotherm, and the enthalpy is based on the mass concentration of NIPA in the copolymer.

of the DF gels was relatively insensitive to temperature, and no VPT was observed over the temperature range covered (see Figure 2). Although there is an appreciable error in the absolute value of the water absorbed that is inherent to this experiment due to sample handling, the changes in the water sorption that occurred at the VPT was significantly greater than the experimental error, so that the temperatures for the VPT, T_{VPT}, are expected to be reasonably accurate.

The VPT of the NF gels was also detected by DSC measurements (see Figure 4). The endotherm is due to the dissociation of water molecules from the amide group that occurs at the VPT. The enthalpy measured for the NIPA gel, 40.1 J/g, is consistent with the range of values reported in the literature, 30.1−39.8 J/g.[50] As with the swelling data, the DSC experiments show that T_{VPT} decreased and the transition became broader with increasing FOSA concentration in the copolymer. The values of T_{VPT} obtained from the two different experiments differed by about 3−5 °C, but the trends in T_{VPT} with FOSA concentration were similar (see Figure 3). The transition enthalpy decreased with increasing FOSA concentration due to the lower water concentration of the swollen gels. Consistent with the swelling measurements, no VPT was observed by DSC measurements for the DF and DMA gels.

The decrease of T_{VPT} is analogous to the depression of the LCST that Ringsdorf et al.[26] reported for the hydrophobic modification of polyNIPA by the copolymerization of NIPA with longer alkyl chain-modified acrylamides and to the decrease of the VPT for HEMA-modified NIPA copolymer gels.[52] There are no published reports of a VPT for polyDMA hydrogels or LCST behavior for polyDMA aqueous solutions. One difference between DMA and NIPA is the absence of an amide proton in DMA. However, poly(*N*,*N*-diethylacrylamide), polyDEA, which also has no amide proton, but which is more hydrophobic than polyDMA, does exhibit a VPT.[59−62] Thus, it would appear that the most logical explanation for the absence of a VPT is simply a result of the more hydrophilic nature of polyDMA and that the temperature of a VPT for an aqueous is too high to be

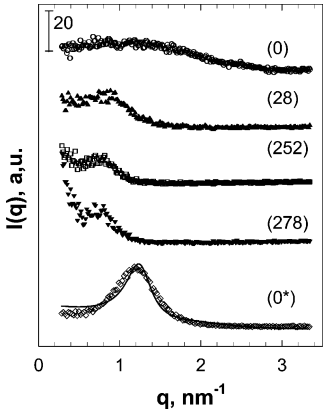

Figure 5. SAXS curves for NF5 as a function of hydration at 10 °C. The numbers in parentheses denote the water concentration in the gel. The curve labeled (0) is the molded film, and the one labeled (0*) represents a film that was dried after swelling with water. The curves were shifted vertically for clarity. The solid curve is the fit of the Griffith et al. hard-sphere model.

observed at ambient pressure. Nevertheless, incorporation of the hydrophobic FOSA into polyDMA neither induced a VPT nor sufficiently lowered T_{VPT} so that it was experimentally accessible.

Small-Angle X-ray Scattering (SAXS). Figure 5 shows the SAXS data for NF5 as a function of hydration at 10 °C, which is below T_{VPT} for that copolymer. The dry NF5 sample exhibited a broad scattering peak due to nanophase separation of the hydrophobic FOSA. The scattering vector for the peak maximum, $q_{max} \sim 1.1$ nm^{-1}, corresponds to a characteristic size in real space of $d = 5.7$ nm ($d = 2\pi/q_{max}$), which most likely represents a correlation length between FOSA nanodomains. Swelling the sample with water shifted the SAXS peak to lower q (increasing d). For 28% water $q_{max} = 0.85$ nm^{-1} ($d = 7.4$ nm), and for 252% water $q_{max} = 0.75$ nm^{-1} ($d = 8.4$ nm). Increasing the water content to 278% had little noticeable effect on the position of the scattering peak. The increase of the spacing between FOSA nanodomains was due to the preferential swelling of the hydrophilic NIPA matrix. For 252% and 278% water sorption, an upturn in the scattering intensity at low q, which was absent for the dry sample, also became evident.

The presence of the scattering peak in the hydrated samples indicated that the nanophase separation of the FOSA domains persisted in the swollen gels, and the upturn in scattering intensity at low q indicated larger sized inhomogeneities in the gel that were absent in the dry copolymer. Large-scale concentration inhomogeneities are commonly observed in chemically cross-linked gels due to fluctuations in the cross-link density.[63−66] The similar observation for the NF gels indicates that large concentration fluctuations of the physical cross-links also occurs and that conclusion is also supported by the nonuniform spatial distribution of FOSA nanodomains, as evident by the broad scattering peak for the dry copolymer. An inhomogeneous distribution of nanodomains, or in this case the physical cross-link junctions for the NF gels, may produce inhomogeneities in the swelling of the gel, as shown schematically in Figure 6. Swelling the copolymer homogenizes to some extent the distribution of inter-FOSA domain spacings, which accounts for the narrowing of the scattering peak. But, in regions where the nanodomain concentration is relatively high, the local swelling of the gel may be lower

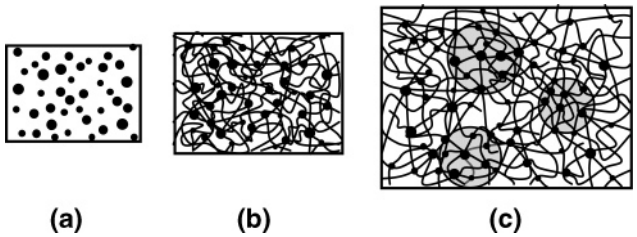

Figure 6. Schematic of the various inhomogeneities in the physical gels as a function of hydration: (a) dry polymer or low hydration—chains form a dense, homogeneous phase (chains are not shown); (b) intermediate hydration—two inhomogeneities: the nanodomains and the water-swollen chain structure; (c) high hydration—three inhomogeneities: nanodomains, water-swollen chain structure, and nanodomain clusters. The black circles represent the FOSA nanodomains that comprise the cross-link junctions of the network. The shaded areas indicate the nanodomain clusters due to the inhomogeneous hydration of the network.

than the global value, and relatively large regions, or clusters, of higher FOSA nanodomain concentration may produce scattering at low q. A more thorough examination of the microstructure of these hydrogels was carried out using small-angle neutron scattering. Those results are discussed, and a model for the microstructure is proposed in a second paper.[57] As will be shown in that paper, the SAXS upturn seen in Figure 5 is actually part of a scattering peak that corresponds to an intercluster spacing.

Figure 5 also shows the SAXS data for the NF5 gel obtained after swelling the dry copolymer with water and then drying it again. The low-q intensity upturn was absent, as it was for the original dry copolymer, but the broad scattering peak was considerably sharper for the hydrated/dried sample and the peak was centered at $q_{max} = 1.2$ nm^{-1} ($d = 5.2$ nm). Thus, the effect of swelling on the microstructure of the molded sample was irreversible and swelling tended to produce a more uniform distribution of inter-nanodomain distances. The perfection of the hydrophobic microstructure upon swelling the gel was probably facilitated by the increased mobility of the chains, and the structure formed under those conditions more closely represents the equilibrium state of the copolymer. That conclusion is supported by the reversibility of the copolymer microstructure (i.e., the SAXS data) upon swelling and deswelling the sample after the initial swelling of the as-molded film.

The size of the FOSA domains in the dry copolymer was estimated by fitting the SAXS data for the sample that was swollen with water and then dried with a polydisperse interacting hard-sphere model proposed by Griffith et al.[67]

$$I(q) = \int_0^\infty P_i^2(q)\, G(\sigma_i)\, \mathrm{d}\sigma_i + \int_0^\infty \int_0^\infty P_i(q)\, P_j(q)\, H_{ij}(q)\, G(\sigma_i)\, G(\sigma_j)\, \mathrm{d}\sigma_i\, \mathrm{d}\sigma_j \quad (2)$$

where P is the scattering amplitude, σ is the particle diameter, $G(\sigma)$ is the particle size distribution function, and $H_{ij}(q)$ is the pair correlation function, with the subscripts referring to the two particles i and j. A Schulz distribution was used because of its mathematical simplicity. The fit is shown in Figure 5 for the 0* sample. The model provided an effective hard sphere radius, r_{eff}, and an effective volume fraction of hard spheres, ϕ_{eff}, which were then used to calculate an average radius of the FOSA-rich nanodomains, $r_0 = 1.8$

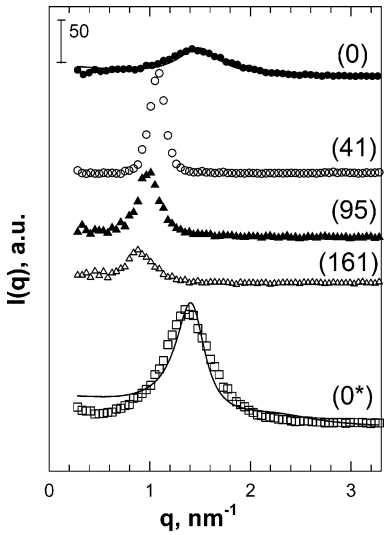

Figure 7. SAXS curves for DF9 as a function of hydration at ~23 °C. The numbers in parentheses denote the water concentration in the gel. The curve labeled (0) is the molded film, and the one labeled (0*) represents a film that was dried after swelling with water. The curves were shifted vertically for clarity. The solid curve is the fit of the eq 2, the hard-sphere model.

nm, using eq 3, which is based on the average volume fraction of FOSA nanodomains ϕ_0

$$r_0 = (\phi_0/\phi_{\text{eff}})^{1/3} r_{\text{eff}} \tag{3}$$

Similarly, a FOSA nanodomain size of $r_0 = 1.6$ nm was determined for the dry NF8 and NF10 copolymers. The hard-sphere model, however, did not adequately fit the scattering data for the dry, as-molded NF5 film or the water-swollen films due to large inhomogenities in the structure of the former and the additional clustering structure indicated by the low-q intensity upturn for the latter samples.

SAXS data for the hydrated DF9 sample are shown in Figure 7. As with the NF5 sample, the SAXS of the dry DF9 showed a broad scattering peak centered at $q_{\max} = 1.44$ nm^{-1} ($d = 4.4$ nm) due to nanophase separation of the FOSA. Also similar to the behavior for the NF gels, when the DF9 was hydrated, the scattering peak sharpened, increased in intensity, and shifted to lower q. At the equilibrium swelling, 161% water, $q_{\max} = 0.9$ nm^{-1} ($d = 7.0$ nm). The dehydrated sample exhibited a scattering peak at $q_{\max} = 1.3$ nm^{-1} ($d = 4.8$ nm), which shows that there was considerable hysteresis in the microstructure of these gels. The SAXS peak for the dehydrated copolymer was narrower and higher in intensity than that for the initial dry sample, which indicated that the dispersion of nanodomains became more uniform after swelling the gel. The fit of the Griffith et al. hard-sphere model to the SAXS data for the DF9 film that was swollen with water and then dried produced a radius of 1.8 nm for the FOSA nanodomains, which is comparable to that in the NF5 copolymers discussed above. The radius of the FOSA nanodomains in the DF copolymers, as calculated from fits of the Griffith et al. hard-sphere model, was affected by FOSA concentration, changing from $r_0 = 1.4$ to 2.1 nm as the FOSA concentration increased from 5 to 22 mol %. The structure of the FOSA nanodomains and the effects of temperature and water content are discussed in more detail in a second paper.[57]

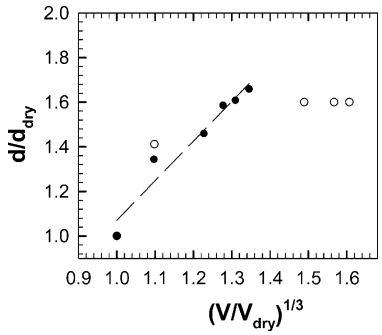

Figure 8. Normalized nanodomain spacing vs the cube root of the normalized volume for (○) NF5 and (●) DF9 as a function of swelling with water.

Table 3. SAXS Parameters of Dry and Hydrated Copolymers

gel ID		DF5	DF9	DF22	NF5	NF8	NF10
dry	$q_{\max}$ nm^{-1}	1.4	1.45	1.55	1.25	1.35	1.45
	d, nm	4.5	4.3	4.1	5	4.7	4.3
gel	d, nm	7.9	7	6.6	8.4	8.1	
	upturn	no	no	no	yes	yes	yes
	water, wt %	330	175	70	300	160	115

The shift of the SAXS peak to lower q upon swelling the gel is due to the increased separation of the nanodomains as the volume of the gel increased. The water presumably only swells the hydrophilic, i.e., alkylacrylamide, phase. That conclusion is supported by the relationship between the characteristic length, d, associated with the SAXS peak and the volume of the gel (see Figure 8). The data in Figure 8 were normalized by the characteristic length and volume of the dry copolymers. If one assumes an affine deformation of the network chains between the cross-links—in this case, between the FOSA nanodomains—which is reasonable if the nanodomain structure was unperturbed by the swelling of the gel with water, the expectation is that "d" should scale with $V^{1/3}$. The agreement between the data and the affine deformation model for the DF gels is good, which indicates that water uniformly swelled those gels. However, the data for the NF gels in Figure 8 deviate from the affine prediction, probably due to an inhomogeneous distribution of the FOSA domains, as evidenced by the scattering peak and the low-q upturn in Figure 5. The absence of a low-q upturn in the intensity for the DF gels, as was observed for the NF gels (e.g., Figures 5 and 7), also supports the conclusion that the nanodomain dispersion in the DF gels was more uniform than in the NF gels.

The SAXS vs water swelling behavior for the other NF and DF gels was similar to that of the NF5 and the DF9 gels. For both NF and DF gels, a scattering peak corresponding to the interdomain spacing of FOSA nanodomains was observed in the dry and hydrated states. The peak shifted to lower q with increasing hydration, corresponding to increased inter-nanodomain spacing. For the NF gels, a distinct intensity upturn became evident at high degrees of swelling. This was attributed to large-scale inhomogeneties in the distribution of FOSA nanodomains. SAXS results for all the NF and DF gels, dry and fully swollen, are summarized in Table 3. In general, the interdomain spacing decreased with increasing FOSA concentration. The interdomain spacing in the dry copolymers scaled roughly as the FOSA concentration to the one-third power, but the number of samples studied was insufficient to get good statistics on that correlation. Still, as a first approxima-

tion, that result would be expected as either the number or size of the nanodomains increased with increasing concentration of the hydrophobic FOSA.

Conclusions

Physically cross-linked, FOSA/*N*-isopropylacrlyalmide (NIPA) copolymer (NF) hydrogels exhibited a volume phase transition (VPT) similar to what is observed for covalently cross-linked NIPA hydrogels. The temperature of the VPT (T_{VPT}) decreased and the transition broadened as the FOSA concentration in the copolymer increased. The decrease of the T_{VPT} was due to the increased hydrophobicity introduced by the FOSA comonomer. The broadening of the transition was probably a consequence of local differences in the hydrophilic/hydrophobic balance of the copolymer due to large inhomogeneities in the microstructure and nonuniform swelling of the NF gels. No VPT has been reported for covalently cross-linked DMA hydrogels, and the introduction of as much as 21.5 mol % of the hydrophobic FOSA comonomer did not produce a VPT in FOSA/*N*,*N*-dimethylacrylamide (DMA) copolymer (DF) hydrogels.

Hydrophobic interactions promoted nanophase separation of the FOSA in both the DF and NF physical gels. The microstructure of these physical gels was significantly different from covalently cross-linked hydrogels in that the cross-link junctions of the physical gels consisted of FOSA nanodomains. In part 2 of this study,[57] a more thorough examination of the gel microstructure will be discussed.

Acknowledgment. We acknowledge the financial support from Petroleum Research Fund of the American Chemical Society (Grant 36649-AC7) and Wesley Jessen Corp.

References and Notes

(1) Emmon, W. D.; Stevens, T. E. U.S. Pat. 4,395,524, 1983.
(2) Turner, S. R.; Siano, D. B.; Bock, J. U.S. Pat. 4,528,348, 1985.
(3) Flynn, C. E.; Goodwin, J. W. In *Polymers as Rheology Modifiers*; Schulz, D. N., Glass, J. E., Eds.; American Chemical Society: Washington, DC, 1991; pp 190−206.
(4) Audibert, A.; Noik, C.; Rivereau, A. U.S. Pat. 6,710,107, 2004.
(5) Yoshida, M.; Kumakura, M.; Kaetsu, I. *J. Macromol. Sci., Chem.* **1980**, *A14*, 555−569.
(6) Park, T. G.; Hoffman, A. S. *Bitechnol. Prog.* **1991**, *7*, 383−390.
(7) Shimizu, S.; Yamazaki, M.; Kubota, S.; Ozasa, T.; Moriya, H.; Kobayashi, K.; Mikami, M.; Mori, Y.; Yamaguchi, S. *Artif. Organs* **1996**, *20*, 1232−1237.
(8) Park, T. G. *Biomaterials* **1999**, *20*, 517−521.
(9) Eremeev, N. L.; Kukhtin, A. V. *Anal. Chim. Acta* **1997**, *347*, 27−34.
(10) Beliayeva, E. A.; Bogdanovskaya, V. A.; Eremeev, N. L.; Kazanskaya, N. F. *Biotekhnologiya* **1999**, *2*, 76−81.
(11) Dong, L.-C.; Hoffman, A. S. *J. Controlled Release* **1990**, *13*, 21−31.
(12) Bae, Y. H.; Okano, T.; Kim, S. W. *Pharm. Res.* **1991**, *8*, 531−537.
(13) Okano, T.; Yoshida, R.; Sakai, K.; Sakurai, Y. In *Polym. Gels: Fundam. Biomed. Appl., [Proc. Int. Symp.]*; DeRossi, D., Ed.; Plenum: New York, 1991.
(14) Yoshida, R.; Sakai, K.; Okano, T.; Sakurai, Y. *Polym. J. (Tokyo)* **1991**, *23*, 1111−1121.
(15) Kaneko, Y.; Yoshida, R.; Sakai, K.; Sakurai, Y.; Okano, T. *J. Membr. Sci.* **1995**, *101*, 13−22.
(16) Yu, H.; Grainger, D. W. *J. Controlled Release* **1995**, *34*, 117−127.
(17) Serres, A.; Baudys, M.; Kim, S. W. *Pharm. Res.* **1996**, *13*, 196−201.
(18) Kaetsu, I.; Uchida, K.; Shiomi, T.; Tamori, A.; Sutani, K. *Proc. Int. Symp. Controlled Release Bioactive Mater.* **1998**, *25*, 880−881.
(19) Zhang, Y.-X.; Da, A.-H.; Hogen-Esch, T. E.; Butler, G. B. *J. Polym. Sci., Part C: Polym. Lett.* **1990**, *28*, 213−218.
(20) Zhang, Y.-X.; Da, A.-H.; Butler, G. B.; Hogen-Esch, T. E. *J. Polym. Sci., Part A: Polym. Chem.* **1992**, *30*, 1383−1391.
(21) Zhang, Y. X.; Huang, F. S.; Hogen-Esch, T. E. In *Macromolecular Complexes in Chemistry and Biology*; Dubin, P., Bock, J., Davis, R. M., Schulz, D. N., Thies, C., Eds.; Springer-Verlag: Berlin, 1994.
(22) Hogen-Esch, T. E.; Amis, E. *Trends Polym. Sci. (Cambridge, U.K.)* **1995**, *3*, 98−104.
(23) Xie, X.; Hogen-Esch, T. E. *Macromolecules* **1996**, *29*, 1734−1745.
(24) Seery, T. A. P.; Yassini, M.; Hogen-Esch, T. E.; Amis, E. J. *Macromolecules* **1992**, *25*, 4784−4791.
(25) Bock, J.; Valint, P. L. J.; Pace, S. J.; Siano, D. B.; Schulz, D. N.; Turner, S. R. In *Water-Soluble Polym. Pet. Recovery, [Proc. Natl. Meet. ACS]*; Stahl, G. A., Schulz, D. N., Eds.; Plenum: New York, 1988.
(26) Ringsdorf, H.; Venzmer, J.; Winnik, F. M. *Macromolecules* **1991**, *24*, 1678−1686.
(27) Priest, J. H.; Murray, S. A.; Nelson, R. J. *Polym. Prepr. (Am. Chem. Soc., Div. Polym. Chem.)* **1986**, *27*, 239−240.
(28) Taylor, L. D.; Cerankowski, L. D. *J. Polym. Sci., Part A: Polym. Chem.* **1975**, *13*, 2551−2570.
(29) Amis, E. J.; Hu, N.; Seery, T. A. P.; Hogen-Esch, T. E.; Yassini, M.; Hwang, F. In *Hydrophilic Polymers: Performance with Environmental Acceptance*; Glass, J. E., Ed.; American Chemical Society: Washington, DC, 1996; Vol. 248, pp 278−302.
(30) Bae, S. S.; Chakrabarty, K.; Seery, T. A. P.; Weiss, R. A. *J. Macromol. Sci., Pure Appl. Chem.* **1999**, *A36*, 931−948.
(31) Li, M.; Jiang, M.; Zhang, Y.-X.; Fang, Q. *Macromolecules* **1997**, *30*, 470−478.
(32) Dusek, K.; Patterson, D. *J. Polym. Sci., Polym. Phys. Ed.* **1968**, *6*, 1209−1216.
(33) Tanaka, T. *Phys. Rev. Lett.* **1978**, *40*, 820−823.
(34) Hirokawa, Y.; Tanaka, T. *J. Chem. Phys.* **1984**, *81*, 6379−6380.
(35) Hirotsu, S.; Hirokawa, Y.; Tanaka, T. *J. Chem. Phys.* **1987**, *87*, 1392−1395.
(36) Inomata, H.; Goto, S.; Saito, S. *Macromolecules* **1990**, *23*, 4887−4888.
(37) Hu, Y.; Horie, K.; Ushiki, H. *Macromolecules* **1992**, *25*, 6040−6044.
(38) Kang, S. I.; Bae, Y. H. *Macromolecules* **2001**, *34*, 8173−8178.
(39) Tanaka, T.; Fillmore, D.; Sun, S.-T.; Nishio, I.; Swislow, G.; Shah, A. *Phys. Rev. Lett.* **1980**, *45*, 1636−1639.
(40) Katayama, S.; Ohata, A. *Macromolecules* **1985**, *18*, 2781−2782.
(41) Hirokawa, Y.; Tanaka, T.; Sato, E. *Macromolecules* **1985**, *18*, 2782−2784.
(42) Amiya, T.; Tanaka, T. *Macromolecules* **1987**, *20*, 1162−1164.
(43) Mamada, A.; Tanaka, T.; Kungwatchakun, D.; Irie, M. *Macromolecules* **1990**, *23*, 1517−1519.
(44) Juodkazis, S.; Mukai, N.; Wakaki, R.; Yamaguchi, A.; Matsuo, S.; Misawa, H. *Nature (London)* **2000**, *408*, 178−181.
(45) Fujishige, S.; Kubota, K.; Ando, I. *J. Phys. Chem.* **1989**, *93*, 3311−3313.
(46) Kubota, K.; Fujishige, S.; Ando, I. *Polym. J. (Tokyo)* **1990**, *22*, 15−20.
(47) Wu, C.; Zhou, S. *Macromolecules* **1997**, *30*, 574−576.
(48) Wu, C. *Polymer* **1998**, *39*, 4609−4619.
(49) Li, Y.; Tanaka, T. *J. Chem. Phys.* **1989**, *90*, 5161−5166.
(50) Otake, K.; Inomata, H.; Konno, M.; Saito, S. *Macromolecules* **1990**, *23*, 283−289.
(51) Hoffman, A. S.; Afrassiabi, A.; Dong, L. C. *J. Controlled Release* **1986**, *4*, 213−222.
(52) Cicek, H.; Tuncel, A. *J. Polym. Sci., Part A: Polym. Chem.* **1998**, *36*, 527−541.
(53) Shibayama, M.; Mizutani, S.-y.; Nomura, S. *Macromolecules* **1996**, *29*, 2019−2024.
(54) Beltran, S.; Hooper, H. H.; Blanch, H. W.; Prausnitz, J. M. *J. Chem. Phys.* **1990**, *92*, 6337.
(55) Beltran, S.; Baker, J. P.; Hooper, H. H.; Blanch, H. W.; Prausnitz, J. M. *Macromolecules* **1991**, *24*, 549−551.
(56) Shibayama, M.; Tanaka, T.; Han, C. C. *J. Chem. Phys.* **1992**, *97*, 6842−6854.
(57) Tian, J.; Seery, T. A. P.; Ho, D. L.; Weiss, R. A. *Macromolecules* **2005**, *38*, 10001−10008.
(58) Grinberg, N. V.; Dubovik, A. S.; Grinberg, V. Y.; Kuznetsov, D. V.; Makhaeva, E. E.; Grosberg, A. Y.; Tanaka, T. *Macromolecules* **1999**, *32*, 1471−1475.

(59) Ilavsky, M.; Hrouz, J.; Ulbrich, K. *Polym. Bull. (Berlin)* **1982**, *7*, 107−113.
(60) Plestil, J.; Ostanevich, Y. M.; Borbely, S.; Stejskal, J.; Ilavsky, M. *Polym. Bull. (Berlin)* **1987**, *17*, 465−472.
(61) Spevacek, J.; Geschke, D.; Ilavsky, M. *Polymer* **2000**, *42*, 463−468.
(62) Lessard, D. G.; Ousalem, M.; Zhu, X. X. *Can. J. Chem.* **2001**, *79*, 1870−1874.
(63) Stein, R. S. *J. Polym. Sci., Polym. Lett. Ed.* **1969**, *7*, 657−660.
(64) Wun, K. L.; Prins, W. *J. Polym. Sci., Polym. Phys. Ed.* **1974**, *12*, 533−543.
(65) Candau, S. J.; Young, C. Y.; Tanaka, T.; Lemarechal, P.; Bastide, J. *J. Chem. Phys.* **1979**, *70*, 4694−4700.
(66) Bastide, J.; Leibler, L. *Macromolecules* **1988**, *21*, 2647−2649.
(67) Griffith, W. L.; Triolo, R.; L., C. A. *Phys. Rev. A* **1987**, *35*, 2200−2206.

MA049475R